5-1-2016

Numerical and Analytical Modeling to Determine Performance Trade-offs in Hydrogel-based pH Sensors

Piyush Dak
Purdue University

Muhammad Ashraful Alam
Purdue University

Dak, Piyush and Alam, Muhammad Ashraful, "Numerical and Analytical Modeling to Determine Performance Trade-offs in Hydrogel-based pH Sensors" (2016). *Birck and NCN Publications.* Paper 1674.
http://dx.doi.org/10.1109/TED.2016.2557233

Numerical and Analytical Modeling to Determine Performance Trade-offs in Hydrogel-based pH Sensors

Piyush Dak, and Muhammad Ashraful Alam, *Fellow*, *IEEE*

***Abstract*— Hydrogel based pH sensors are promising candidates for implantable sensors due to their low-cost and biocompatibility. Despite their commercial potential and numerous theoretical/experimental reports, the trade-offs between different performance parameters are not well understood, and explicitly stated. In this work, we develop a numerical and analytical framework to show that there is a fundamental trade-off between the performance parameters *i.e.* sensitivity/dynamic range vs. response-time/response-asymmetry in hydrogel sensors under constrained swelling conditions. Specifically, we consider the effect of the gel parameters, such as the ionizable group density (N_f) and its dissociation constant (K_a), on the sensor performance. We show that improvement of sensitivity/dynamic range leads to degradation in response time/symmetry and therefore, a compromise must be made to optimize device performance.**

***Index Terms*— Hydrogel, pH Sensor, Sensitivity, Response Time**

I. Introduction

Decorated with capture probes, stimuli-sensitive hydrogels are three-dimensional cross-linked polymeric materials which swell/shrink depending on analyte (chemical/biomolecule) and environmental conditions such as pH [1]–[6], ionic concentration [1], temperature [5], glucose [7]–[9], antigen [10] , etc. These materials have been explored for numerous biomedical applications [11], such as, chemical/biomolecule sensing [1]–[7], [10], [12], contact lenses [13], drug delivery [14], tissue engineering [15], etc. Hydrogels are biocompatible (they do not trigger an immune response), encouraging their recent use in active implantable sensors [6], [7], [16] to continuously monitor vital health parameters.

Hydrogel sensors can be operated either in *free swelling* mode (FSM) or *constrained-swelling* mode (CSM). When a FSM sensor is exposed to an analyte solution, the hydrogel volume changes significantly. This change can be monitored by optical [17]–[19], oscillating [20], or conductimetric [21], [22] sensors. In CSM sensors, on the other hand, the hydrogel is confined between a rigid porous membrane and a semi-rigid deformable membrane [2], [6], [7], [23], see, Fig. 1(a). The porous layer allows the analyte (*i.e.* proton) to diffuse into the hydrogel, but it does not deform due to the change in hydrogel pressure. Instead, when the analyte concentration changes, hydrogel pressure deforms the deformable membrane below. The magnitude of the pressure (ΔP) depends on several factors, such as the composition of the polymer comprising the hydrogel, the density and affinity of the capture probes to analyte (*i.e.* protons), and the environmental conditions such as temperature, ionic concentration, etc. The small deflection of the membrane due to change in pressure can then be read by various transducers such as capacitive sensor [6], [7] and piezoelectric sensor [4], [5], [24].

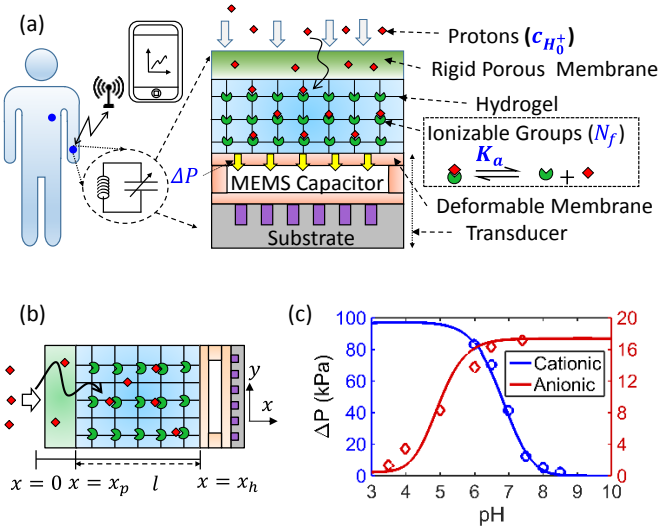

Fig. 1 (a) Schematic of a Hydrogel based Wireless Implantable Biochemical Sensor System: The sensor (blue) is implanted into a human body. The sensor is composed of an LC resonator with a hydrogel sandwiched between a rigid porous membrane and a deformable membrane. The hydrogel is pendent with the ionizable groups (with density, N_f and dissociation constant, K_a) which are responsive to analyte (say, proton) molecules. As the analyte concentration changes, the pressure exerted by hydrogel on deformable membrane changes which can be wirelessly detected, (b) 1D approximation for simulation of hydrogel sensor, (c) Experimental validation of static pressure change as a function of pH for cationic and anionic hydrogel. Lines represent the numerical simulation results and circle/polygon represent experimental data obtained from Ref. [1] and [6], respectively.

Several groups have reported numerical, analytical and experimental studies regarding the kinetics and steady-state response of *free-swelling* hydrogels. For example, Grimshaw *et al.* [25] and De *et al.* [26], [27] have reported experimental and numerical studies on free swelling kinetics of polyelectrolyte gel (without the porous membrane). Lesho *et al.* [28] reported an analytical formulation supported by

This work was supported by the National Science Foundation Center through the Nano-Engineered Electronic Devices.
The authors are with the School of Electrical and Computer Engineering, Purdue University, West Lafayette, IN 47907 USA (e-mail: pdak @purdue.edu; alam@purdue.edu).

experiments to determine swelling kinetics of unconstrained gels. Ballhause *et al.* [29] have numerically investigated the swelling dynamics based upon chemical stimulation due to change in ionic concentration. Kang *et al.* [30] have developed a chemo-electro-mechanical model to investigate pH dependent free-swelling of hydrogels.

In contrast, the CSM sensors are relatively new and have not been analyzed as extensively. Herber *et al.* [1] and Lei *et al.* [6] experimentally studied the pressure generated due to pH. Guenther *et al.* [4], [5], [24] and Trinh *et al.* [31] reported analytical models to determine the response of a gel under constrained conditions. Despite these significant advances both in multi-physics modeling and experiments, the key design trade-offs between the signal (characterized by sensitivity (S) and dynamic range (ΔpH_{range})) and time response (characterized by response time (τ) and symmetry of the response) are not clearly understood. Obviously, it would be difficult to design and optimize a hydrogel sensor unless these tradeoffs are explicitly specified.

The two important attributes that govern the sensor response to pH changes are: a) The concentration of ionizable groups (N_f) [1], and b) The affinity of the ionizable group to the protons which is determined by its acid dissociation constant (K_a). Both these design variables can be changed by using either a different ionizable group (characterized by a different K_a [32]) and/or changing N_f during hydrogel preparation.

An ideal pH sensor should sense the proton density ($c_{H_0^+}$) with high precision (determined by sensitivity), within a specific period of time (determined by response time), and it should do so over a broad pH range (determined by dynamic range). Also, it is preferable to have a sensor which shows symmetric response for rise and fall in the pH value. However, our findings suggest that these performance parameters are correlated and the improvement of one leads to the degradation of the other. In this work, we provide a systematic numerical and analytical framework *to interpret and highlight these trade-offs for a gel characterized by* (N_f, K_a). Our analysis yields the following important conclusions regarding the trade-off between sensitivity (S)/ dynamic range (ΔpH_{range}) and response time (τ)/response symmetry of CSM sensors:

1. *Trade-off dictated by density of fixed ionic groups, N_f*: While S and ΔpH_{range} of the sensor improve with increasing N_f, τ degrades.
2. *Trade-off dictated by dissociation constant*[1]*, pK_a:* While S is highest for choice of $pK_a \sim pH$ (*i.e.* desired pH range of operation), τ degrades and the sensor response is asymmetric.

The paper is divided into following sections: In Section 2, we provide a description of the model system and describe the numerical and analytical model. Section 3, we use these models to highlight the trade-offs associated between different performance parameters such as signal (sensitivity/dynamic range) and time response (response time/symmetry of response). Finally, we conclude with Section 4 by summarizing the essence of the work.

[1] Note, the acid dissociation constant (K_a) and $pK_a = -\log_{10}(K_a)$ are inter-related and have been used inter-changeably throughout the manuscript. Similarly, the concentration of protons ($c_{H_0^+}$) is expressed in terms of the pH ($= -\log_{10}(a_{H^+} c_{H_0^+}) \approx -\log_{10}(c_{H_0^+})$), where a_{H^+} is the activity factor of protons.

II. Model System

1. Device Description

A general scheme for use of CSM sensor in detection of analyte concentration [6], [7], [23] is shown in Fig. 1(a). The sensor can be implanted in the body for continuous monitoring of analyte concentration (say, protons). The recognition element is analyte responsive hydrogel pendent with fixed ionizable (anionic/cationic) molecules with a density, N_f and acid dissociation constant, K_a. The hydrogel is constrained between a rigid porous membrane (top) and a transducer (bottom). The porous membrane can be made from a biocompatible material, for example Al_2O_3 [33]. The change in the analyte concentration brings about a change in the capacitance of the micro-electromechanical system (MEMS) sensor due to the deformation of the flexible membrane. This sensor can be integrated with an inductor to form a LC resonator. The change in resonance frequency reflects the concentration of analyte in the sample, and can be read wirelessly using a receiver (for example, a smartphone).

2. Numerical Framework

A generic hydrogel layer is composed of both anionic and cationic ionizable groups to sense protons. The anionic groups are represented as HA, and their deprotonated (anionic *i.e.* charged form) is given by A^-. The cationic groups are represented as HB^+ and their deprotonated (neutral form) is given by B. For example, for a cationic group $R-NH_2$, $B \equiv R-NH_2$ and $HB^+ \equiv R-NH_3^+$. The protons (shown in red diamonds) enter from left into the rigid porous membrane and diffuse into the hydrogel to reach the transducer surface (see, Fig. 1(b). Due to change in proton concentration, the ionized state of ionizable groups in the hydrogel changes. This brings a change in concentration of salt ions which leads to osmotic pressure on the transducer.

The concentration of the protons (c_{H^+}) in hydrogel is determined by time-dependent self-consistent solution of Poisson (Eq. A1), chemical (Eq. A6-A11) and continuity equations (Eq. A12). The model equations and symbol descriptions are listed in ATable1 and ATable2, respectively. Briefly, we make the following assumptions:

a) The area of the sensor (y-z plane) is much larger than the thickness (x-direction), therefore 1D analysis (see, Fig. 1(b)) is appropriate.
b) Sensor operates in isochoric conditions, so that the change in the thickness of the hydrogel is negligible,
c) The acid-base reactions are faster compared to the diffusion of protons [25], [26], so that chemical equilibrium is established almost instantaneously. Activity factor for all ions is assumed to be 1,

d) Ionic concentration (c_s) is much higher than $c_{H_0^+}$. Therefore, the movement of salt ions is much faster than protons [27].
e) For simplicity, the diffusion coefficient of protons in hydrogel ($D_{H^+,\text{gel}}$) and porous membrane ($D_{H^+,\text{por}}$) are assumed to be same as in pure solvent (D_{H^+}). This approximation is true for small polymer volume fraction in hydrogel and large pore size in porous membrane. If pore size is small and/or polymer fraction large, the diffusion constants need to be appropriately modified [34], [35].
f) For simplicity, we assume that internal strains are small, so that the density of ionizable groups, N_f remains uniform during the sensing operation. If the internal strains are large, our model must be generalized by inclusion of mechanical deformation equations for a more accurate analysis [36].

The solution of the equations provide the time and space dependent concentration of the ionic species (salt ions, protons and hydroxyl ions). The time dependent osmotic pressure ($P(t)$) induced due to the change in concentration of ions is determined by (see, Eq. A13):

$$P(t) = \sum_i (c_i - c_{i0})\, RT \tag{1}$$

where, c_i is the time-dependent concentration of i^{th} ionic species at the hydrogel and transducer interface, c_{i0} is its corresponding concentration in the *pH* solution, R is universal gas constant and T the absolute temperature.

Subsequently, $P(t)$ is used to evaluate different performance parameters such as *sensitivity (S), dynamic range (ΔpH_{range}), response time (τ) and symmetry of response*. The sensitivity is defined as the change in osmotic pressure (ΔP) per unit change in pH. We define the dynamic range as the range of pH for which the sensitivity decreases by half[2] from its maximum value (S_{max}). And, finally we define the response time of the sensor as the time required for the pressure to reach 90% (rise time, τ_{rise}) of the peak value or time required for the pressure to decrease by 90% (fall time, τ_{fall}) from the peak value. The response is symmetric if $\tau_{rise} = \tau_{fall}$.

Numerical model presented in this section is validated with the experimental data obtained from Herber *et al.* [1] and Lei *et al.* [6]. Fig. 1(c) shows the comparison of the simulated steady state pressure (lines) as a function of pH with the experimental data (symbols) for cationic and anionic gels. The results are easily explained: The uncharged groups (B) in cationic gels are protonated (HB^+) at low pH values and exert pressure on the deformable membrane. As pH increases, the fraction of protonated groups decrease and hence the pressure decreases. In contrast, anionic gels are neutral (HA) at low pH values and they become negatively charged (A^-) as pH is increased. This leads to an increase in repulsive force and hence an increase in pressure.

To summarize, this subsection discussed the numerical framework for relating the gel parameters (N_f, K_a) to the performance parameters. In next subsection, we discuss the analytical framework to relate these gel parameters to S and τ.

3. Analytical Framework

To understand the essence/origin of the tradeoff, we consider the response of a hydrogel to a small change in pH. First, we determine S in terms of (N_f, K_a) using analytical analysis, and then we relate it to τ to determine the performance trade-off.

To determine S, we relate the pressure change to the gel parameters (N_f, K_a). Invoking the charge neutrality (see, Eq. A1) in steady state at the hydrogel/transducer interface (see, Fig 1(b)) *i.e.* $x = x_h$, we get,

$$\rho_{net} = q(c_{Na^+} - c_{Cl^-} + c_{H^+} - c_{OH^-}) + \rho_F = 0 \tag{2}$$

where, c_i are the concentrations of ionic species i and ρ_F is the fixed charge density (see, Eq. A3) due to ionizable groups. Since, $[H^+]$ and $[OH^-]$ concentrations are negligible, Eq. (2) becomes,

$$q(c_{Na^+} - c_{Cl^-}) + \rho_F = 0 \tag{3}$$

The concentration of $[Na^+]$ and $[Cl^-]$ ions can be related to potential, ψ_d at $x = x_p$ (called Donnan potential) using Eq. A4, *i.e.*

$$c_{Na^+} = c_s\lambda, \quad c_{Cl^-} = c_s/\lambda \tag{4}$$

where, $\lambda = \exp\left(-\frac{q\psi_d}{k_B T}\right)$ and c_s is the ionic concentration.

Considering only anionic gels with ionizable density, $N_a = N_f$ and using Eq. A6-A8, we get,

$$\rho_F = -qc_{A^-} = -qN_f/(1 + c_H^+/K_a) \tag{5}$$

If potential ψ_d is small, $c_{H^+}(x = x_p) \approx c_{H_0^+}$ (see, Eq. A5). Using Eq. 3-5, we get,

$$\lambda^2 - \alpha\,\lambda - 1 = 0 \tag{6}$$

where, $\alpha = \left(N_f/c_s\right)/\left(1 + \frac{c_{H_0^+}}{K_a}\right)$.

Since, the concentration of H^+ and OH^- are small compared to salt ions, therefore, we can ignore their contributions to osmotic pressure. The pressure increase at the "transducer/hydrogel interface" is then given by (using Eq. 1, 4 and 6),

$$P \approx RT\left(\lambda + \frac{1}{\lambda} - 2\right)c_s = RTc_s\,(\sqrt{\alpha^2 + 4} - 2) \tag{7}$$

The sensitivity, S is given by,

$$S = \frac{dP}{dpH} \approx \alpha \frac{N_f^2}{\sqrt{N_f^2 + \beta^2}} \tag{8}$$

where, $\alpha = 2.3RT\frac{\eta}{(1+\eta)^2}$, $\eta = 10^{-pH+pK_a}$ and $\beta = 2c_s(1 + \eta)$. Eq. 8 suggests that as N_f increases, S also increases. This is because with increase in N_f, ρ_F (see, Eq. 5) increases, and hence the concentration of ions which exert osmotic pressure increases.

Now that we know S as a function of gel parameters (N_f, pK_a), we relate response time (τ) to the parameters (N_f, pK_a).

[2] The choice of 0.5 for dynamic range is arbitrary, and would be defined by the required application. However, the dependencies discussed are true in general and can be applied to any value chosen for the dynamic range.

If the diffusion through the top rigid porous membrane is fast as compared to diffusion through hydrogel, τ is limited only due to transport in hydrogel. Therefore, τ can be expressed as [25], [28],

$$\tau = \gamma \frac{4l^2}{\pi^2 D_{eff}}, \qquad D_{eff} = D_{H^+} / \left(1 + \frac{N_f K_a}{(K_a + c_{H^+})^2}\right) \quad (9)$$

where, l is the hydrogel thickness (see, Fig. 1(b)) and D_{H^+} is the diffusion constant of protons (c_{H^+}) in the hydrogel membrane, and γ is a proportionality constant. The protons moving through the hydrogel membrane are slowed due to instantaneous quasi-equilibrium established between the protons and the ionizable groups (see, Ref [37] for more information), this results in reduced effective diffusion constant (D_{eff}) and an increased τ.

Eq. 9 suggests that τ scales as l^2, the thickness of the hydrogel. However, for a sensor to work, there must be sufficient strain at the transducer, and this ultimately puts a minimum limit to the hydrogel thickness. For a given l, τ decreases as N_f decreases or as K_a shifts away from c_{H^+}.

Neglecting 1 in Eq. 9 and rearranging, we get $N_f = k\tau$ where $k = \frac{\pi^2 D_{H^+}}{4\gamma l^2} \frac{(K_a + c_{H^+})^2}{K_a}$. Therefore, by substituting $N_f = k\tau$ in Eq. 8, we get S vs. τ trade-off equation,

$$S = a\tau^2 / \sqrt{\tau^2 + \tau_0^2} \quad (10)$$

where, $a = 2.3\ RT\ k \frac{\eta}{(1+\eta)^2}$ and $\tau_0 = 2(1+\eta)c_s/k$.

Trade-off highlighted by Eq. 10 is one of the *key conclusions* of the paper. It suggests that an increase in S is correlated to an increase in τ. Therefore, a compromise must be made between the two performance parameters for CSM sensors.

Limitations of analytical analysis: Although the analytical analysis provides some intuition into the trade-off, a numerical model (as discussed earlier) is essential to a) include the effect of Donnan potential, ψ_d (which can be considerable for large N_f), b) account for diffusion through the porous membrane, c) interpret the asymmetry in time response for large pH changes (since, c_{H^+} is a function of space and time), d) explain the effect of ionic concentration on the response time.

III. Results and Discussions

In this section, we use the numerical model to determine the response of the sensor on gel parameters (N_f, pK_a), and use analytical model to interpret the trade-offs between the performance parameters. We suggest ways to improve the signal and time response and show that the improvement of one performance parameter (such as sensitivity/dynamic range) leads to degradation of the other (response time/symmetry in response). Therefore, a trade-off must be considered between performance parameters for optimal design of the sensor.

1) *Role of Ionizable Group Density (N_f):*

N_f is a design variable that can be changed during hydrogel preparation. As discussed in Section II, N_f not only affects the response time but also sensitivity. In addition, N_f affects the dynamic range and apparent pK_a (point of maximum sensitivity). In this subsection, we will discuss the role of N_f in dictating these performance parameters and associated trade-offs between them.

Fig. 2(a) shows the numerical simulation of normalized sensitivity as a function of $pH - pK_a$ for two different ratios of anionic group densities (N_f) to the salt concentration (c_s). Two observations can be made: First, as N_f increases, the maximum sensitivity point *i.e.* apparent pK_a (pK_{app}) shifts to right. The shift in pK_{app} point reflects the change in Donnan potential due to ionized fixed charges. Second, the dynamic range (ΔpH_{range}) increases from ΔpH_1 to ΔpH_2. Fig. 2(b) shows the dependence of ΔpH_{range} and $\Delta pK_a = pK_{app} - pK_a$ on N_f/c_s ratio. The ΔpH_{range} increases by almost 0.7 pH units as N_f/c_s ratio increases from 0.1 to 10. Further, pK_{app} deviates from the real pK_a by almost 1 unit for very large anionic density ($N_f = 1M$ for $c_s = 100mM$). To summarize, if N_f is large, the dynamic range is high and pH at which sensor is most sensitive (pK_{app}) shifts away from pK_a.

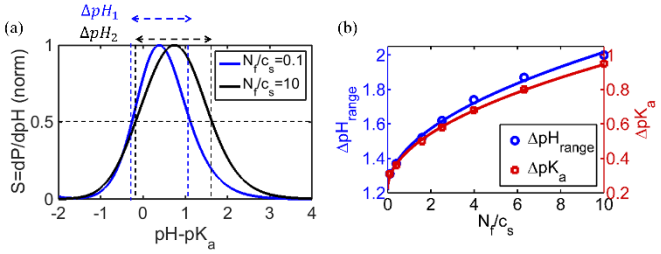

Fig. 2(a) Normalized change in pressure as a function of pH for two different ratios of anionic density (N_f) to salt concentrations (c_s). The sensitivity is maximum near the pK_a (*i.e.* apparent pK_a) of the anionic groups. (b) Change of dynamic range (ΔpH_{range}) and the difference between the apparent pK_a and real pK_a (ΔpK_a) as a function of the N_f/c_s ratio. As the ratio increases, the dynamic range of the sensor increases. Symbols are the numerical simulation results and the lines are guide to eye.

Fig. 3 (a) shows the numerically simulated pressure change as a function of time for a small change in pH (from 5 to 5.1, with $pK_a = 5$) for two different densities of the anionic group *i.e.* $25\ mM$ and $100\ mM$ respectively. While the pressure change (ΔP) increases as N_f changes from $25\ mM$ to $100\ mM$, it takes longer to reach the saturation pressure value.

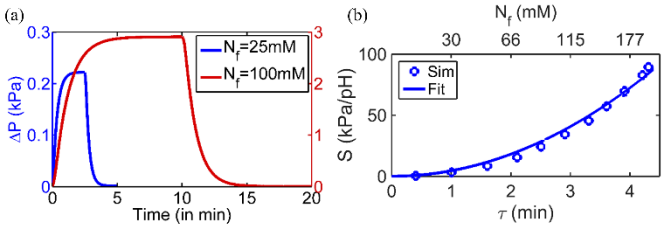

Fig. 3(a) Change in pressure as a function of time for two different anionic densities upon pH step from 5 to 5.1 ($pK_a = 5$), (b) Tradeoff between sensitivity and response time: As the sensitivity increases, the response time also increases. Symbols represent numerical simulation and line represents fit using Eq. 10. Hydrogel thickness is $20\ \mu m$, Porous membrane thickness is $5\ \mu m$.

Fig. 3(b) shows the trade-off between sensitivity ($S = \Delta P/\Delta pH$) and response time (τ) as N_f is varied. While S increases with N_f, τ increases as well, leading to a slower sensor response. This trend is in agreement with the experiments by Herber *et. al.* [1] where the authors increased the relative composition of monomer dimethylaminoethyl methacrylate (DMAEMA) in their hydrogel preparation. Therefore, a compromise must be made between S and τ.

Interestingly, despite of the simplifying assumptions made in derivation of Eq. 10, the analytical result (line) in Fig. 3(b) matches the numerical result (symbols) quite well with appropriate fitting parameters a and τ_0 (see, ATable 3). Numerical simulations show that neglecting Donnan potential overestimates sensitivity by ~25% and response time by ~30%. Also, while Eq. (9) suggests that τ is independent of salt concentration (c_s), detailed numerical simulations (not shown) show that τ can vary by almost 2-3 times as c_s changes from $20\ mM$ to $200\ mM$. Therefore, although all the qualitative trends and trade-offs as a function of various sensor parameters are explained by analytical model in Sec IIC, a numerical simulation is essential for accurate prediction of the response time and sensitivity.

To summarize, Fig. 2(b) and Fig. 3(b) highlight the importance of N_f in dictating the trade-off between different performance parameters. While S and ΔpH_{range} both improve as N_f increases, τ degrades. The requirement to have a reasonable τ puts a maximum limit on N_f.

2) *Role of dissociation constant (pK_a) of ionizable groups:*

The choice of anionic/cationic ionizable group (characterized by a pK_a) can significantly affect S and τ. In this subsection, we consider the choice of ionizable group for a pH sensor designed to operate near $pH = 5$ (as an illustrative example). However, the implications are general and the same analysis follows for other pH values.

2.1) Time response for small pH changes ($\Delta pH \ll log_{10}(e)$): Fig. 4 (a) shows the numerically simulated change in pressure as a function of time for three different anionic groups for the pH change, ΔpH by 0.1 unit at base $pH = 5$ (*i.e.* desired pH operation). Two observations can be made: First, the response of the sensor is symmetric (rise time is same as fall time). Second, τ is maximum for anionic group with pK_a close to the desired range of operation of the device ($pH = 5$).

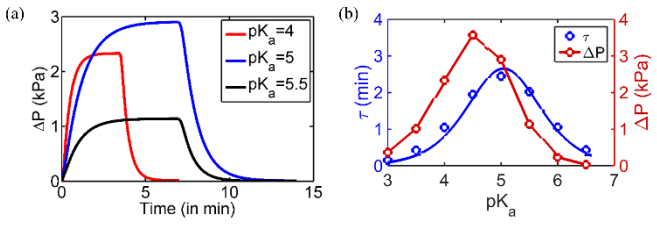

Fig. 4 (a) Change in pressure as a function of time for a pH change from $5 \rightarrow 5.1 \rightarrow 5$ for anionic groups with different pK_a values, (b) The change in response time (τ) and pressure change (ΔP) as a function of pK_a. While S is high for pK_a close to the desired pH range, τ is also high. Blue and red symbols represent numerical simulation result, and blue line represent fit using Eq. 9. Red line is a guide to eye. Hydrogel thickness is 20 μm, Porous membrane thickness is 5 μm, $N_f = 100\ mM$.

Fig. 4(b) shows the numerically simulated (symbols) response time and pressure change as a function of pK_a of the ionizable group. Analytical expression for response time, $\tau \approx a\, K_a/(K_a + c_{H^+})^2$ (see, Eq. 9) (line) fits the numerical result quite well with appropriate fitting parameter a (see, ATable 3), and average c_{H^+}. The figure illustrates that while sensitivity ($S \sim \Delta P$) is maximum when $pK_a \sim pH$, the response of the sensor is slowest. Therefore, a trade-off must be considered between S and τ for appropriate design of the sensor.

2.2) Time response for large pH changes ($\Delta pH \geq log_{10}(e)$): Fig. 5(a) shows the simulated response of the sensor for a pH change from $4 \rightarrow 5 \rightarrow 4$ for anionic groups with different pK_a. Two observations can be made: *a)* The sensitivity is higher when pK_a is close to the base pH value, *b)* The sensor response is asymmetric *i.e.* $\tau_{rise} \neq \tau_{fall}$.

Fig. 5(b) shows the numerically simulated (symbols) τ_{rise}, τ_{fall} and sensitivity ($S \sim \Delta P$) as a function of the pK_a. Analytical expression for response time, $\tau \approx a\, K_a/\left(K_a + c_{H^+,\text{eff}}\right)^2$ (see, Eq. 9) (blue/green line) fits the numerical result for both τ_{rise} and τ_{fall} quite well with appropriate fitting parameters (see, ATable3). Note, that we use effective proton concentration $c_{H^+,\text{eff}}$ (obtained from fit) instead of c_{H^+}, since the concentration of protons (c_{H^+}) increase/decreases by a factor of 10 as the pH change is large. The figure illustrates that the sensor response is symmetric and faster only for choice of anionic groups whose pK_a is far off from the base pH value. However, S degrades in such a scenario, and therefore a trade-off must be considered.

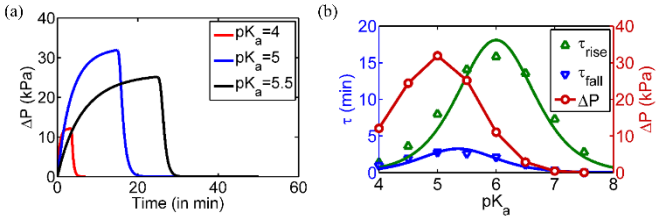

Fig. 5 (a) Change in pressure as a function of time for large changes in pH values (from $pH = 4 \rightarrow 5 \rightarrow 4$) for different choice of anionic groups (*i.e.* different $pK_a's$), (b) The rise (τ_{rise}) and fall (τ_{fall}) time and the change in pressure as a function of the pK_a. While the sensor is most sensitivity for pK_a close to the base pH value (*i.e.* $pH = 5$), the response time is also high. Further, the asymmetry (*i.e.* $\tau_{rise} \neq \tau_{fall}$) is high when pK_a is close to the desired pH range. The symbols show numerical simulation and smooth lines show the fit to the analytical expression (Eq. 9) for τ_{rise} and τ_{fall}.

To summarize, Fig. 4(b) and Fig. 5(b) highlight the importance of ionizable group (*i.e.* pK_a) in dictating the trade-off between S and τ, for sensors with both small and large pH variations. While S is maximized if $pK_a \sim pH$, τ degrades and the asymmetry (for large pH changes) increases. Therefore, a compromise must be made between S and τ or symmetry of response for appropriate design of the sensor.

IV. CONCLUSIONS

Biocompatibility of hydrogel encourages its use in implantable biochemical sensors, however, the design of the hydrogel based sensors is non-trivial and requires a careful theoretical analysis for optimizing different performance parameters such as signal (sensitivity/dynamic range) and time response (response time/symmetry of sensor response). Our analysis demonstrates that there is a fundamental trade-off between performance parameters of a CSM hydrogel sensor. Specifically,

1. If a high sensitivity and a high dynamic range is desirable (for applications where sluggishness of the response is not a primary concern), the density of ionizable group (N_f) should be high and the ionizable group should be selected such that its pK_a is close to the desired pH range.
2. On the other hand, if fast response time and symmetry is an essential prerequisite, N_f should be low and ionizable group should be selected such that its pK_a is shifted away from the desired pH range.

Our analysis suggests opportunity for improving dynamic range of the sensor. The high sensitivity near pK_a suggests that the dynamic range can be improved by using hydrogels prepared with more than one type of ionizable group. The technical feasibility of this approach would be a fruitful research direction for hydrogel sensors.

APPENDIX

ATable1. Equations for numerical simulation

Poisson Equation: $-\frac{\partial}{\partial x}\left(\varepsilon(x)\frac{\partial\psi(x,t)}{\partial x}\right)=\rho_{net}(x,t)=\rho_M(x,t)+\rho_F(x,t)$	(A1)
$\rho_M(x,t)=q(c_{Na^+}-c_{Cl^-}+c_{H^+}-c_{OH^-}),$	(A2)
$\rho_F(x,t)=q(c_{HB^+}-c_{A^-})$	(A3)
$c_{Na^+}=c_s\exp\left(-\frac{q\psi(x,t)}{kT}\right), c_{Cl^-}=c_s\exp\left(\frac{q\psi(x,t)}{kT}\right)$	(A4)
$c_{OH^-}=K_w/c_{H^+}$ $c_{H^+}=c_{H_0^+}\exp\left(-\frac{q\psi_d}{kT}\right)$ (in steady state)	(A5)
Chemical Equilibrium:	
Anionic Ionizable Groups: $HA \underset{}{\overset{K_a}{\rightleftarrows}} H^+ + A^-$	(A6)
$N_a=c_{HA}+c_{A^-}$ (A7) $\quad K_a=c_{H^+}c_{A^-}/c_{HA},$ (A8)	
Cationic Ionizable Groups: $HB^+ \underset{}{\overset{K_b}{\rightleftarrows}} H^+ + B$	(A9)
$N_b=c_{HB^+}+c_B$ (A10) $\quad K_b=c_{H^+}c_B/c_{HB^+},$ (A11)	
Continuity Equation: $\frac{\partial c_{H^+,tot}}{\partial t}=-\frac{\partial}{\partial x}\left(J_{\mathrm{H^+,drift}}+J_{\mathrm{H^+,diff}}\right)$ $J_{\mathrm{H^+,drift}}=-\mu_{H^+}(x)c_{H^+}\frac{\partial\psi}{\partial x}, \quad J_{\mathrm{H^+,diff}}=-D_{H^+}(x)\frac{\partial c_{H^+}}{\partial x}$ $c_{H^+,tot}=c_{H^+}+c_{HA}+c_{HB^+}$	(A12)
Osmotic Pressure: (see, Ref. [27]) $c_{gel}=c_{Na^+,gel}+c_{Cl^-,gel}+c_{H^+,gel}+c_{OH^-,gel}$ $P(t)=RT(c_{gel}-c_{sol})$	(A13)
$c_{gel}=c(x=x_h,t),\ c_{sol}=c(x=0,t)$	
Boundary Conditions (see, Fig. 1(b)): $\psi(x=0,t)=0;\ c_{H^+}(x=0,t)=10^{-pH}$ $(d\psi/dx)_{x=x_h}=0\ ;(dc_{H^+}/dx)_{x=x_h}=0$	(A14)

ATable2. Description of Symbols

Symbol	Quantity
τ	Response time
τ_{rise} or τ_{fall}	Time required for pressure to reach 90% of the peak pressure value or decrease by 90% of the peak value.
S	Sensitivity of the sensor
ΔpH_{range}	Dynamic range of the sensor
l	Thickness of hydrogel membrane
$B,\ A^-$	Deprotonated form of cationic and anionic groups, respectively. Example: $B\equiv R-NH_2, A^-\equiv R-COO^-$
HB^+, HA	Protonated form of cationic and anionic groups, respectively.
c_{H^+}, c_{OH^-} c_{Na^+}, c_{Cl^-}	Concentration of proton, hydroxyl, sodium and chloride ions at position x and time t, respectively.
$c_{H_0^+}$	Concentration of protons to be detected in sample solution
c_s	Ionic concentration of the solution
ρ_M	Mobile ion charge density
ρ_F	Fixed charge density due to protonation/deprotonation of the ionizable groups in hydrogel
$K_a,\ K_b$	Acid dissociation constant for anionic and cationic groups, respectively in hydrogel
K_w	The ionization constant of water at absolute temperature T
pK_a, pK_b	$pK_a=-\log_{10}(K_a), pK_b=-\log_{10}(K_b)$
N_a, N_b	The density of ionizable anionic and cationic groups, respectively
N_f	The density of the ionizable groups (anionic or cationic)
D_{eff}	Effective diffusion coefficient of protons in hydrogel after accounting for reaction with ionizable groups
ψ_d	Donnan Potential *i.e.* potential at $x=x_h$ in steady state

ATable3. List of fitting parameters for match of analytical expressions to numerical model

Fig., Plot	Fitting Parameters
3(b), S vs. N_f	$\alpha=0.6$ kPa/mM, $\beta=180.4$ mM
3(b), S vs. τ	$a=16420\ kPa$ min^{-1}, $\tau_0=3629$ min
4(b), τ_s vs. pK_a	$a=9.5\times10^{-2}$ min mM
5(b), τ_{rise} vs. pK_a	$a=7.24\times10^{-2}$ min mM, $c_{H^+,\mathrm{eff}}=10^{-3}$mM
5(b), τ_{fall} vs. pK_a	$a=5.83\times10^{-2}$ min mM, $c_{H^+,\mathrm{eff}}=4.5\times10^{-3}$ mM

ACKNOWLEDGEMENTS

The authors would like to thank Prof. B. Ziaie, A. Ebrahimi, H. Jiang, and X. Jin for useful discussions.

REFERENCES

[1] S. Herber, J. Eijkel, W. Olthuis, P. Bergveld, and A. Van Den Berg, "Study of chemically induced pressure generation of hydrogels under isochoric conditions using a microfabricated device," *J. Chem. Phys.*, vol. 121, no. 6, pp. 2746–2751, 2004.

[2] M. Lei, A. Baldi, T. Pan, Y. Gu, R. A. Siegel, and B. Ziaie, "A hydrogel-based wireless chemical sensor," in *17th IEEE International Conference on Micro Electro Mechanical Systems. Maastricht MEMS 2004 Technical Digest*, Jan. 2004, pp. 391–394.

[3] G. Gerlach, M. Guenther, J. Sorber, G. Suchaneck, K.-F. Arndt, and A. Richter, "Chemical and pH sensors based on the swelling behavior of hydrogels," *Sensors Actuators B Chem.*, vol. 111–112, pp. 555–561, Nov. 2005.

[4] M. Guenther, D. Kuckling, C. Corten, G. Gerlach, J. Sorber, G. Suchaneck, and K. Arndt, "Chemical sensors based on multiresponsive block copolymer hydrogels," *Sensors Actuators B Chem.*, vol. 126, no. 1, pp. 97–106, Sep. 2007.

[5] M. Guenther, G. Gerlach, and T. Wallmersperger, "Non-linear

Effects in Hydrogel-based Chemical Sensors: Experiment and Modeling," *J. Intell. Mater. Syst. Struct.*, vol. 20, no. 8, pp. 949–961, 2009.

[6] M. Lei, A. Baldi, E. Nuxoll, R. A. Siegel, and B. Ziaie, "Hydrogel-based microsensors for wireless chemical monitoring.," *Biomed. Microdevices*, vol. 11, no. 3, pp. 529–38, Jun. 2009.

[7] M. Lei, A. Baldi, E. Nuxoll, R. A. Siegel, and B. Ziaie, "A hydrogel-based implantable micromachined transponder for wireless glucose measurement.," *Diabetes Technol. Ther.*, vol. 8, pp. 112–122, Feb. 2006.

[8] C. Zhang, M. D. Losego, and P. V Braun, "Hydrogel-Based Glucose Sensors: Effects of Phenylboronic Acid Chemical Structure on Response," *Chem. Mater.*, vol. 25, no. 15, pp. 3239–3250, Aug. 2013.

[9] C. Zhang, G. G. Cano, and P. V Braun, "Linear and fast hydrogel glucose sensor materials enabled by volume resetting agents.," *Adv. Mater.*, vol. 26, no. 32, pp. 5678–83, Aug. 2014.

[10] T. Miyata, N. Asami, and T. Uragami, "A reversibly antigen-responsive hydrogel.," *Nature*, vol. 399, no. 6738, pp. 766–9, Jun. 1999.

[11] A. S. Hoffman, "Hydrogels for biomedical applications," *Adv. Drug Deliv. Rev.*, vol. 54, no. 1, pp. 3–12, Jan. 2002.

[12] N. A. Peppas and C. D. Bures, "Glucose-Responsive Hydrogels," *Encyclopedia of Biomaterials and Biomedical Engineering*., Abingdon, UK.: Taylor & Francis, 2008, pp. 1163–1173

[13] P. C. Nicolson and J. Vogt, "Soft contact lens polymers: an evolution," *Biomaterials*, vol. 22, no. 24, pp. 3273–3283, Dec. 2001.

[14] T. R. Hoare and D. S. Kohane, "Hydrogels in drug delivery: Progress and challenges," *Polymer (Guildf).*, vol. 49, no. 8, pp. 1993–2007, Apr. 2008.

[15] K. Y. Lee and D. J. Mooney, "Hydrogels for Tissue Engineering," *Chem. Rev.*, vol. 101, no. 7, pp. 1869–1880, Jul. 2001.

[16] T. Tokuda, M. Takahashi, K. Uejima, K. Masuda, T. Kawamura, Y. Ohta, M. Motoyama, T. Noda, K. Sasagawa, T. Okitsu, S. Takeuchi, and J. Ohta, "CMOS image sensor-based implantable glucose sensor using glucose-responsive fluorescent hydrogel.," *Biomed. Opt. Express*, vol. 5, no. 11, pp. 3859–70, Nov. 2014.

[17] M. F. McCurley, "An optical biosensor using a fluorescent, swelling sensing element," *Biosens. Bioelectron.*, vol. 9, no. 7, pp. 527–533, Mar. 1994.

[18] Z. Shakhsher, W. R. Seitz, and K. D. Legg, "Single Fiber-Optic pH Sensor Based on Changes in Reflection Accompanying Polymer Swelling," *Anal. Chem.*, vol. 66, no. 10, pp. 1731–1735, May 1994.

[19] M. T. V. Rooney and W. Rudolf Seitz, "An optically sensitive membrane for pH based on swellable polymer microspheres in a hydrogel," *Anal. Commun.*, vol. 36, no. 7, pp. 267–270, Jan. 1999.

[20] A. Richter, A. Bund, M. Keller, and K.-F. Arndt, "Characterization of a microgravimetric sensor based on pH sensitive hydrogels," *Sensors Actuators B Chem.*, vol. 99, no. 2–3, pp. 579–585, May 2004.

[21] N. F. Sheppard, R. C. Tucker, and S. Salehi-Had, "Design of a conductimetric pH microsensor based on reversibly swelling hydrogels," *Sensors Actuators B Chem.*, vol. 10, no. 2, pp. 73–77, Jan. 1993.

[22] N. F. Sheppard Jr., M. J. Lesho, P. McNally, and A. Shaun Francomacaro, "Microfabricated conductimetric pH sensor," *Sensors Actuators B Chem.*, vol. 28, no. 2, pp. 95–102, Aug. 1995.

[23] P. Dak and M. A. Alam, "A Predictive Model for Hydrogel based Wireless Implantable Bio-chemical Sensors," in *73st Device Research Conference*, 2015.

[24] M. Guenther, G. Gerlach, and T. Wallmersperger, "Piezoresistive biochemical sensors based on hydrogels," *Microsyst. Technol.*, vol. 16, no. 5, pp. 703–715, 2010.

[25] P. E. Grimshaw, J. H. Nussbaum, A. J. Grodzinsky, and M. L. Yarmush, "Kinetics of electrically and chemically induced swelling in polyelectrolyte gels," *J. Chem. Phys.*, vol. 93, no. 6, p. 4462, 1990.

[26] S. K. De, N. R. Aluru, B. Johnson, W. C. Crone, D. J. Beebe, and J. Moore, "Equilibrium swelling and kinetics of pH-responsive hydrogels: models, experiments, and simulations," *J. Microelectromechanical Syst.*, vol. 11, no. 5, pp. 544–555, Oct. 2002.

[27] S. K. De and N. R. Aluru, "A chemo-electro-mechanical mathematical model for simulation of pH sensitive hydrogels," *Mech. Mater.*, vol. 36, no. 5–6, pp. 395–410, 2004.

[28] M. J. Lesho and N. F. Sheppard, "A method for studying swelling kinetics based on measurement of electrical conductivity," *Polym Gels Netw*, vol. 5, no. 6, pp. 503–523, 1998.

[29] D. Ballhause and T. Wallmersperger, "Coupled chemo-electro-mechanical finite element simulation of hydrogels: I. Chemical stimulation," *Smart Mater. Struct.*, vol. 17, no. 4, p. 045011, 2008.

[30] B. Kang, Y. D. Dai, X. H. Shen, and D. Chen, "Dynamical modeling and experimental evidence on the swelling/deswelling behaviors of pH sensitive hydrogels," *Mater. Lett.*, vol. 62, no. 19, pp. 3444–3446, 2008.

[31] Q. Thong Trinh, G. Gerlach, J. Sorber, and K.-F. Arndt, "Hydrogel-based piezoresistive pH sensors: Design, simulation and output characteristics," *Sensors Actuators B Chem.*, vol. 117, no. 1, pp. 17–26, Sep. 2006.

[32] D. D. Perrin, B. Dempsey, and E. P. Serjeant, *pKa prediction for organic acids and bases*. Chapman and Hall, 1981.

[33] D. S. Finch, T. Oreskovic, K. Ramadurai, C. F. Herrmann, S. M. George, and R. L. Mahajan, "Biocompatibility of atomic layer-deposited alumina thin films.," *J. Biomed. Mater. Res. A*, vol. 87A, no. 1, pp. 100–6, Oct. 2008.

[34] L. Pisani, "Simple Expression for the Tortuosity of Porous Media," *Transp. Porous Media*, vol. 88, no. 2, pp. 193–203, Feb. 2011.

[35] B. Amsden, "Solute Diffusion within Hydrogels. Mechanisms and Models," *Macromolecules*, vol. 31, no. 23, pp. 8382–8395, Nov. 1998.

[36] S. R. Eisenberg and a J. Grodzinsky, "The kinetics of chemically induced nonequilibrium swelling of articular cartilage and corneal stroma.," *J. Biomech. Eng.*, vol. 109, no. February 1987, pp. 79–89, 1987.

[37] A. J. Grodzinsky, *Fields, Forces, and Flows in Biological Systems*, 1st Editio. Garland Science, 2008.

Piyush Dak received the B.Tech. & M. Tech. degree in Engineering Physics from IIT Bombay, Mumbai, India in 2010. He is currently pursuing the Ph.D. degree with the School of Electrical and Computer Engineering at Purdue University, West Lafayette, IN, USA.

His current research interests include modeling, simulation and characterization of electronic devices for memory and healthcare applications.

Muhammad Ashraful Alam (M'96–SM'01–F'06) received the Ph.D. degree from Purdue University in 1995.

After spending a decade at Bell Laboratories in Murray Hill, NJ, working laser dynamics, crystal growth, and CMOS reliability, he returned to Purdue in 2004, where he currently holds the Jai N Gupta Professorship of Electrical Engineering. His current research includes physics, performance limits, and novel concepts in biosensors, solar cells, and transistors.